Glass formation in a multicomponent Zr-based alloy by mechanical attrition and liquid undercooling

A. Sagel, R. K. Wunderlich, J. H. Perepezko,[a] and H.-J. Fecht[b]
Institute of Metal Physics and Technology, Technical University Berlin, D-10623 Berlin, Germany

(Received 15 October 1996; accepted for publication 26 November 1996)

The synthesis of a multicomponent $Zr_{60}Al_{10}Ni_9Cu_{18}Co_3$ glass by mechanical alloying has been investigated using thermal and structural analysis and compared with a metallic glass produced by liquid undercooling. The solid-state amorphization reaction is preceded by rapid solution of smaller solute atoms in the Zr matrix with a concomitant reduction in grain size to 10 nm at the amorphization onset. A fully amorphous mechanically alloyed sample shows relaxation compared to a sample synthesized by liquid cooling probably due to removal of residual inhomogeneities on the scale of the nanocrystal size at amorphization. While the kinetic pathways for the two synthesis methods differ, the relaxed amorphous phases from each method exhibit identical thermodynamic properties. © *1997 American Institute of Physics.* [S0003-6951(97)01705-1]

Glasses can be obtained by several routes including (i) incorporating static disorder into a crystalline phase mixture through solid-state processes or (ii) freezing in dynamic disorder through sufficient undercooling of the liquid at a composition outside the polymorphous melting temperature T_0.[1] The equivalence of the amorphous state achieved by the two pathways is of interest in terms of the evolution of the amorphization (am) processes. This issue is addressed in the present study by examining the structural and thermal properties of a multicomponent $Zr_{60}Al_{10}Ni_9Cu_{18}Co_3$ glass, which is representative of a wider class of new alloys.[2] Multicomponent Zr-based alloys have recently been shown to produce bulk glassy metals at liquid cooling rates as low as 1–500 K/s.[3,4] While all of the factors responsible for the easy glass formation have not been fully identified, it is evident that multicomponent interactions can be important.[5,6] In the present work, powder samples synthesized by mechanical alloying (MA) are compared with liquid-quenched samples of the same composition.

Elemental powders of 99.99% purity with the composition $Zr_{60}Al_{10}Ni_9Cu_{18}Co_3$ were mechanically alloyed under a high purity Ar atmosphere in a Spex ball mill with a powder-to-ball ratio of 6:1.[7] After 36 h of ball milling, the oxygen and the Fe content were determined by EDX to be approximately 1 at. %. Liquid-quenched samples with about 50 μm thickness were also produced in a splat quenching device. X-ray diffraction spectra (XRD) were obtained with an Enraf Nonius goniometer with a large-angle position sensitive detector (Inel CPS 120). Thermal analysis was performed with a Perkin Elmer DSC-7 in Al pans under purified Ar atmosphere. Temperature and specific heat calibrations were carried out with melting point and heat of fusion of indium and zinc.

The XRD spectra taken at different stages of the milling process are characterized by the disappearance of the elemental Ni, Co, Cu, and Al peaks and a shift in the Zr (101) peak to higher 2Θ values in Fig. 1(a). From observations on binary powder mixtures,[7,8] this is indicative of the subsequent dissolution of Ni, Cu, Co, and Al in the Zr matrix with a concomitant shrinkage of the hcp lattice. Figure 1(a) shows, in addition, the average Zr grain diameter as evaluated with the Scherrer formula based on the Zr (101) peak. The final grain size of 10 nm is reached after 5 h milling time. After 7 h milling time, a broad background in the XRD spectra indicates the onset of amorphous phase formation.

The appearance of the broad am halo in the XRD spectra is correlated clearly with the observation of a glass transition in a differential scanning calorimetry (DSC) trace. The final product of the am reaction in the multicomponent powder is established by the constancy of structural measures such as the 2Θ position and width of the am halo together with thermal characteristics such as the glass transition temperature T_g, height of endothermic step at T_g, width of the glass transition δT_g, defined as the difference between the onset

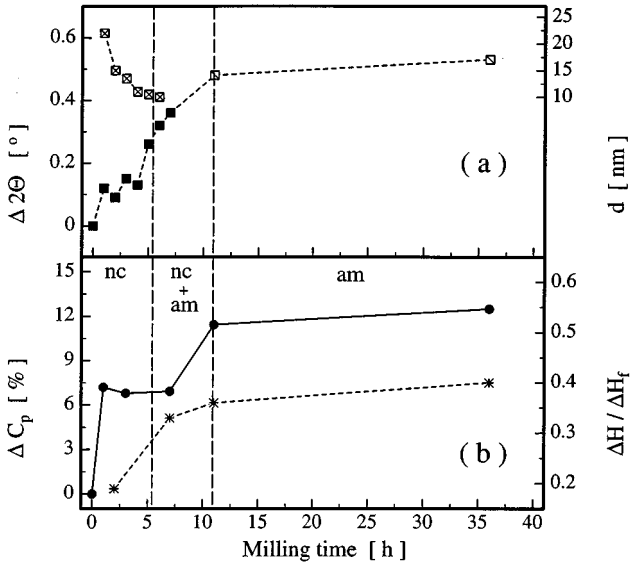

FIG. 1. (a) Grain diameter of Zr (⊠) and shift in the 2Θ position of the hcp Zr (101) peak (■) and of the first am halo (⧅) as a function of milling time. (b) Change in the specific heat $C_p - C_p^{\text{ideal}}/C_p^{\text{ideal}} = \Delta C_p$ of powder specimen (●) and integrated heat release $\Delta H(*)$ normalized to the latent heat, ΔH_f, as a function of milling time.

[a]Permanent address: Department of Materials Science and Engineering, University of Wisconsin–Madison, 1509 University Avenue, Madison, WI 53706.
[b]Electronic mail: fecht@emmi.physik.tu-berlin.de

 0003-6951/97/70(5)/580/3/$10.00

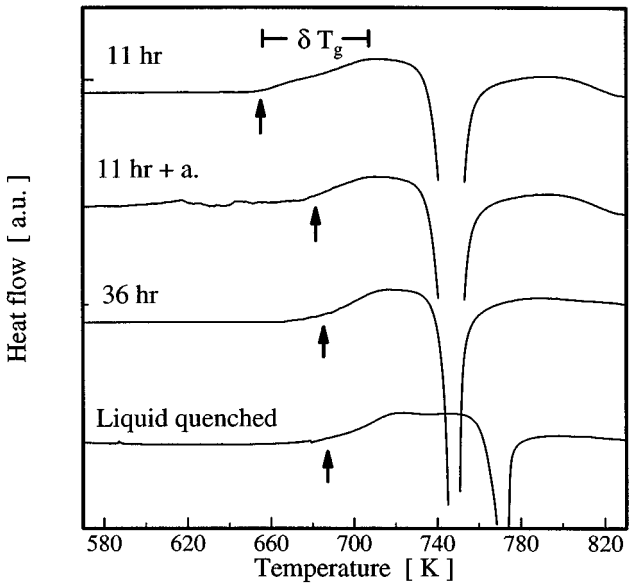

FIG. 2. DSC traces of 11 h, 11 h+annealed, 36 h mechanically milled samples, and rapidly quenched splat with a heating rate of 10 K/min.

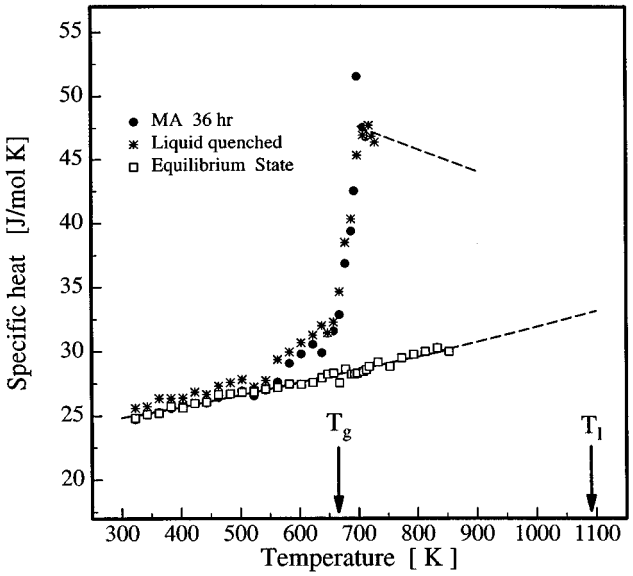

FIG. 3. Specific heat as a function of temperature of 36 h milled powder (●), liquid-quenched sample (∗), and equilibrated sample (□). The milled powder and liquid-quenched samples are amorphous while the equilibrated sample is fully crystalline.

and the maximum of glass transition as shown in Fig. 2, and the crystallization enthalpy at a given heating rate. DSC thermograms from powder specimens after 11 and 36 h milling time and from a liquid-quenched alloy are given in Fig. 2 and show a similar T_g between the 36 h milled specimen and the liquid-quenched glass for a heating rate of 10 K/min. Moreover, XRD spectra do not reveal any structural difference indicating the similarity of the amorphous state of the powder and the liquid quenched specimen with regard to the above criteria.

In order to investigate further the evolution of the am phase, DSC measurements were performed at different stages of the milling process. Figure 1(b) shows the change in specific heat ΔC_p at 320 K of the powder specimen as compared to an ideal solution of the pure elements and the integrated exothermic heat release ΔH up to 870 K normalized to the latent heat, ΔH_f, as a function of milling time. The overall dependence of ΔC_p and $\Delta H/\Delta H_f$ on milling time correlates well with that of the Zr (101) peak position in Fig. 1(a). The first increase of 7% in C_p for milling times 0–3 h is mainly the result of the intermixing reaction of the fast moving alloy species[9] with the Zr matrix together with a possible small contribution from the formation of grain boundaries in the nanoscaled structure. For milling times <10 h the enthalpy release consists of contributions due to grain growth as well as the amorphization reaction.[10] The second break in the C_p increase after a milling time of 8 h is correlated with the onset of the amorphization reaction. For milling times >11 h the final value of the C_p increase at 12% is similar to the observations made on binary Zr–Al alloys.[7] This is in accordance with measurements of the total released enthalpy showing a fraction of the am phase $>92\%$ for 11 h milling time as compared with the final am specimen after 36 h milling time where $\Delta H/\Delta H_f$ reaches 0.4, similar to that of the liquid-quenched sample for the same heating rate.

The DSC thermograms in Fig. 2, taken with a heating rate of 10 K/min, show an increase in T_g as function of milling time from 650 K for the 11 h milled sample to 685 K for the final am phase. It is worthwhile noting that the T_g of the 11 h milled sample is close to that for glassy binary Zr–Ni alloys in the composition range 60–80 at. % Zr.[11] Moreover, the width of the glass transition δT_g decreases as a function of milling time as demonstrated in Fig. 2. Usually, δT_g is about 10–20 K for a given alloy composition.[12] For a multicomponent alloy synthesized from elemental powders, separate local regions can enter the amorphous state at different compositions within the glass forming range and yield a broadened δT_g, which is about 40 K for the 11 h milled sample. Continued milling can serve to homogenize the sample to yield a narrowing of δT_g and an increase in T_g as supported by the 36 h milled sample. A similar effect on δT_g and T_g can be produced by thermal annealing as observed in the 11 h sample after annealing at 650 K in Fig. 2. This compositional relaxation effect on T_g can be opposite to the usual structural relaxation induced by thermal annealing, which yields a lowering of T_g.[13]

Temperature-dependent specific heat measurements, shown in Fig. 3, were performed with the 36 h milled powder, the splat-quenched alloy and a crystallized specimen (equilibrated at 873 K for four days). The powder and liquid-quenched specimens were annealed at (T_g-40 K) for 2 h for relaxation before measurement. At temperatures below T_g the specific heats of both specimens agree very well and, in fact, coincide at T_g. As a further probe of the thermal stability and relaxation behavior of different pathways to the am state, continuous heating experiments are useful. For example, in Fig. 4 a kinetics analysis of the crystallization reaction in the liquid-quenched and the MA samples yields equivalent energetics with an activation energy of 3.6 eV. It is useful to note that, in this case, both Arrhenius and Kissinger plots[14] [where ln (heating rate/T_c^2) is plotted against $1/T_c$] yield similar activation energies. This value is close to

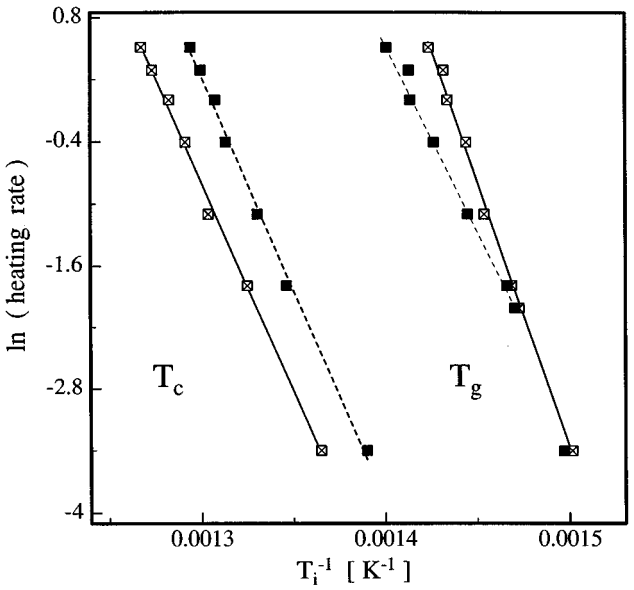

FIG. 4. Arrhenius plot for heating rate dependence of T_g and T_c for the 36 h milled powder (■) and liquid-quenched sample (⊠), unrelaxed.

that reported in binary Zr–Ni glasses,[11] implying that the diffusive processes for the long range solute partitioning involved in crystallization are similar. For the heating rate dependence of T_g an Arrhenius plot is suitable for a limited range.[12] From Fig. 4 there is a divergence in behavior above 10 K/min that offers some insight into the characteristic relaxation scales. For example, for heating rates of $\leqslant$10 K/min, the MA sample behavior merges with that for the liquid-quenched sample indicating a similar relaxation state. Indeed, at the merging point of 10 K/min, which corresponds to a characteristic time of about 10^2 s, the reported diffusivity in amorphous Zr–Al–Cu–Ni alloys (10^{-19}–10^{-20} m^2/s)[15] implies a diffusional distance comparable to the nearest-neighbor separation (i.e., 0.3 nm). For heating ranges $>$10 K/min, the relaxation scales of the samples diverge. From the activation energy of 3.7 eV obtained from the MA sample data in Fig. 4 and reported prefactor,[15] a diffusional scale of 7–9 nm is indicated for the MA sample with heating rates 10–100 K/min. It is interesting that this scale is comparable to the nanocrystal size at the onset of amorphization during MA, indicating that a residual inhomogeneity persists that can be relaxed by annealing. In fact, this has been confirmed by examining the heating rate dependence for a relaxed MA sample. Moreover, the size scale of mixing reflects the effectiveness of ball milling for alloying reactions since the dissolution of 30 μm elemental powders in the 36 h MA samples indicates a ''mechanically enhanced'' diffusivity of at least 10^{-15} m^2/s. Lastly, it is also evident that for a continued decrease in the heating rate, the T_g values will depart the trend in Fig. 4 and will asymptotically approach the ideal glass transition temperature that is evaluated as T_0=640 K based upon analysis of the measured enthalpies and specific heats for the alloy. The apparent structural deviation responsible for the diverging heating rate dependence of T_g can not be clearly identified by standard XRD analysis, but does indicate that the states for the unrelaxed liquid-quenched and am-powder samples as identified by T_g above 10 K/min and XRD are not fully equivalent.

In summary, the amorphous state in a $Zr_{60}Al_{10}Ni_9Cu_{18}Co_3$ alloy has been synthesized by both mechanical alloying of elemental powders and liquid undercooling. Based upon standard XRD and thermal diagnostics (i.e., 2Θ peak position and T_g) the amorphous phase of the 36 h MA sample is similar to that for the liquid-quenched sample. Moreover, the enthalpy of crystallization from the undercooled liquid corresponds to about 40% of the enthalpy of fusion for both types of samples. However, relaxation kinetics measurements expose differences between the two sample types, which can be related to a residual inhomogeneity in the MA sample. In fact, during the alloying reaction that is induced by ball milling, the continued grain size refinement is one measure of the extent of reaction and the spatial extent of the mixing process that can be reflected in residual compositional inhomogeneities. Therefore, although the details of the respective pathways for the MA sample and liquid-quenched alloy are different, the relaxed amorphous phase for each case appears to be similar.

The financial support from the Deutsche Agentur für Raumfahrtangelegenheiten (DARA Grant No. 50 WM 94-31-4), Deutsche Forschungsgemeinschaft (Grant No. Fe 313/6-2), and Alexander von Humboldt Foundation [Senior Research Award Fellowship for one of the authors (J.H.P.)], as well as helpful discussions with Professor A. L. Greer (Cambridge University) and Professor W. L. Johnson (Cal. Tech.) are gratefully acknowledged. The authors are most grateful to Professor K. Samwer (University of Augsburg) for help in providing the splats.

[1] H. J. Fecht and W. L. Johnson, Nature (London) **334**, 50 (1988).
[2] A. Inoue, T. Zhang, and T. Masumoto, Mater. Trans. JIM **36**, 391 (1995).
[3] A. Inoue, T. Zhang, and T. Masumoto, Mater. Trans. JIM **31**, 17 (1990).
[4] A. Peker and W. L. Johnson, Appl. Phys. Lett. **63**, 2342 (1993).
[5] T. Zhang, A. Inoue, and T. Masumoto, Mater. Trans. JIM **32**, 1005 (1991).
[6] S. G. Klose, P. Frankwicz, and H. J. Fecht, Mater. Sci. Forum (in press).
[7] H. J. Fecht, G. Han, Z. Fu, and W. L. Johnson, J. Appl. Phys. **67**, 1744 (1990).
[8] E. Ma and M. Atzmon, Phys. Rev. Lett. **67**, 1126 (1991).
[9] R. B. Schwarz and W. L. Johnson, Phys. Rev. Lett. **51**, 415 (1983).
[10] H. Schroeder, K. Samwer, and U. Köster, Phys. Rev. Lett. **54**, 197 (1985).
[11] Z. Altounian, T. Guo-hua, and J. O. Strom-Olsen, J. Appl. Phys. **54**, 3111 (1983).
[12] H. Baxi and T. B. Massalski, Mater. Sci. Eng. **97**, 291 (1988).
[13] A. L. Greer, in *Rapidly Solidified Alloys, Processes, Structures, Properties, Applications*, edited by H. H. Liebermann (Marcel Dekker, New York, 1993), p. 269.
[14] H. E. Kissinger, Anal. Chem. **29**, 1702 (1957).
[15] U. Köster, J. Meinhardt, S. Roos, and H. Liebertz, Appl. Phys. Lett. **69**, 179 (1996).